Pulse phase variations of the X–ray spectral features in the radio-quiet neutron star 1E 1207–5209

S. Mereghetti, A. De Luca, P.A. Caraveo

Istituto di Astrofisica Spaziale e Fisica Cosmica,
Sezione di Milano "G.Occhialini" - CNR
v.Bassini 15, I-20133 Milano, Italy
sandro@mi.iasf.cnr.it

W. Becker

Max Planck Institut für Extraterrestrische Physik, Giessenbachstrasse,
Postfach 1312, D-85740, Garching, Germany

R. Mignani

European Southern Observatory, Karl Schwarzschild Strasse 2,
D-85740, Garching, Germany

G.F. Bignami

Agenzia Spaziale Italiana, v. Liegi 26, Roma, I-00198, Italy
and Università degli Studi di Pavia

ABSTRACT

We present the results of an *XMM-Newton* observation of the radio-quiet X–ray pulsar 1E 1207–5209 located at the center of the shell-like supernova remnant G 296.5+10.0 . The X–ray spectrum is characterized by the presence of two phase-dependent absorption lines at energies ∼0.7 keV and ∼1.4 keV. Moreover, these broad spectral features have significant substructure, suggesting that they are due to the blending of several narrower lines. We interpret such features as evidence for an atmosphere containing metals and a magnetic field value of a few 10^{12} G, consistent with the observed spin-down rate $\dot{P}=(1.98\pm0.83)\times10^{-14}$ s s^{-1}. Since 1E 1207–5209 is the only X–ray emitting pulsar showing evidence of such features, we tentatively link them to the unique combination of age and energetics that characterize this object. We suggest that a young age and a low level of magnetospheric activity are favorable conditions for the detection of atomic spectral features from metals in neutron star atmospheres, which would be either blanketed by a thin layer of accreted hydrogen in older objects or masked by non-thermal processes in young energetic pulsars.

Subject headings: Stars: neutron; X–ray: stars;

1. Introduction

The thermal emission from the surface of a neutron star traces the star's cooling history. Its study can thus provide invaluable information on the poorly known equation of state of matter at super-nuclear densities and on physical processes in strong magnetic fields. Satellite observations carried out in the last decade have clearly shown the thermal origin of the soft X–ray emission (∼0.1-3 keV) from a handful of middle-aged radio pulsars (Becker & Trümper 1997) as well as from several radio-quiet neutron stars (Caraveo, Bignami & Trümper 1996; Treves et al. 2000).

It is expected that the presence of an atmosphere on the neutron star surface distort the emerging radiation by altering the blackbody energy distribution and introducing absorption features (see, e.g., Zavlin & Pavlov 2002 for a recent review). Fits with atmospheric models generally yield emitting regions compatible with standard neutron star dimensions, thus providing indirect evidence for the presence of an atmosphere. However, until recently no convincing evidence for the absorption features predicted by these models was found, thus leaving substantial uncertainty on the atmospheric composition and magnetic field.

Here we report on an *XMM-Newton* observation of the radio-quiet neutron star 1E 1207–5209 . Previous X–ray, optical and radio observations (Bignami et al. 1992, Mereghetti et al. 1996, Vasisht et al. 1997) strongly suggested a neutron star nature for this source, located close to the geometrical center of the shell-like supernova remnant G 296.5+10.0 (Roger et al. 1988). This was confirmed by the discovery of fast X–ray pulsations with period P=0.424 s (Zavlin et al. 2000). A subsequent measurement (at the $\lesssim 2\sigma$ level) of a positive period derivative $\dot{P} = (2.0^{+1.1}_{-1.3}) \times 10^{-14}$ s s^{-1} (Pavlov et al. 2002a) results in a large discrepancy between the pulsar's characteristic age $\tau_c \equiv \frac{P}{2\dot{P}} = 200 - 900$ kyrs and the age of 7 kyrs (with a factor 3 uncertainty) estimated for the associated SNR (Roger et al. 1988).

Our *XMM-Newton* data show the presence of broad absorption features at ∼0.7 and ∼1.4 keV in the spectrum of 1E 1207–5209 . Such features have been independently discovered in data from the *Chandra* satellite (Sanwal et al. 2002). The high throughput of the *XMM-Newton* telescope, coupled to the good spectral and timing resolution of the European Photon Imaging Camera (EPIC) instrument, allow us to show that the lines have a significant substructure, which varies with the phase of the pulsar.

2. Data Analysis and Results

The *XMM-Newton* observation of 1E 1207–5209 started on December 23, 2001 at 19:13 UT and lasted 28.4 ks. We concentrate here on data obtained with the EPIC instrument, which consists of two MOS CCD detectors (Turner et al. 2001) and a PN CCD instrument (Strüder et al. 2001), for a total collecting area $\gtrsim 2500$ cm^2 at 1.5 keV.

The PN camera was operated in Small Window mode in order to have a time resolution (6 ms) adequate to study the pulsations without sacrificing the imaging, while both MOS CCDs were in the Full Frame mode (2.6 s resolution). All the detectors used the Medium thickness filter. All the data were processed with the *XMM-Newton* Science Analysis Software (SAS Version 5.3). After screening to remove time intervals of high proton background which affected the MOS data, and correcting for the dead time, we obtained net exposure times of 18.7 ks, 22.3 ks and 24.8 ks in the PN, MOS1 and MOS2 respectively.

1E 1207–5209 was clearly detected at a position consistent with previous measurements (Mereghetti et al. 1996), with net count rates (0.3–3 keV) of 1.352±0.008 counts s^{-1} and 0.362±0.004 counts s^{-1}, respectively in the PN and in each MOS.

A circular extraction region with radius 40″ was used for the timing and spectral analysis of the PN data. The background shows a slight intensity gradient across the chip. We verified that using background regions at different positions did not affect significantly the best fit parameters (the source count rate is ∼30 times greater than that of the background in the 0.3–3 keV range). We therefore finally used for the background spectral extraction a box of dimensions $4' \times 2'$ located to the north of the source.

For both MOS cameras we used a circular source extraction region (radius 40″) and the background spectrum was estimated from a concentric annulus with radii 75″ and 200″. This region is entirely contained in the central chip and is not affected by contamination from the internal Si-K fluorescence, largely present near the CCD edges.

2.1. Timing Analysis

For the timing analysis we used only the PN counts with pattern 0-4 and with energy in the range 0.2-2.5 keV. The times of arrival were converted to the Solar System Barycenter and folded, with 8 phase bins, in a range of trial periods around the expected value. This gave a significant detection of the pulsation with a maximum χ^2=110 at P=424.131 ms. To determine more accurately the period value we fitted the χ^2 versus trial period curve with the appropriate $sinc^2$ function, and computed the error on P using the relation between

maximum χ^2 and uncertainty derived by Leahy (1987). This resulted in our best estimate of P = 424.13084±0.00046 ms. For an independent assessment of the period uncertainty, we generated artificial data sets with the same properties (duration, number of counts, pulsed fraction, etc...) of our observation and analyzed them in the same way. The difference between the derived and the true period was found to have a Gaussian distribution with $\sigma = 5 \times 10^{-7}$ s, thus confirming the above estimate of the period uncertainty.

The folded light curve is nearly sinusoidal, with a ∼8% pulsed fraction. A comparison of the light curves at different energies (Fig. 1) does not show significant shape variations. In particular, we do not confirm the phase shift of ∼0.4–0.5 reported by Pavlov et al. (2002a) between the profiles in the 0.3–1 keV and 1–1.7 keV energy bands. Comparison between the *XMM-Newton* period and that measured in January 2000 with *Chandra* (as reported in the re-analysis of Pavlov et al. 2002a) yields a period derivative $\dot{P}$=(1.98±0.83)×10^{-14} s s^{-1}.

2.2. Spectral Analysis

All spectral modeling was done with XSPEC V11 and using the most recent EPIC response matrices [1]. For the PN analysis we used both single and double events in the 0.3–3 keV energy range (we checked *a posteriori* that the results do not change by using only single events). The spectra were binned to have at least 40 counts per channel and to over-sample by a factor 3 the instrumental energy resolution.

As found by Sanwal et al. (2002), fits with single-component models (power law, thermal bremsstrahlung, blackbody) gave unacceptable results (χ^2/dof > 4.4, dof=81) due to the presence of broad absorption features at ∼0.7 and ∼1.4 keV. For completeness, we also tried the atmospheric models available in the XSPEC spectral fitting package, although they refer to weakly magnetized neutron stars (B $\lesssim 10^9 - 10^{10}$ G) and might not be appropriate in the case of 1E 1207–5209 , where the pulsations and the measured $\dot{P}$ testify the presence of a higher magnetic field (B∼ 3×10^{12} G). Hydrogen-atmosphere models (Zavlin, Pavlov & Shibanov 1996), which do not predict lines in the observed energy range, gave residuals very similar to those of the blackbody model, but, as expected, a lower temperature (kT∼0.09 keV, as measured by an observer at infinity) and a larger emitting region. Models implying atmospheres with solar abundance or iron composition (Gänsicke, Braje & Romani 2002) gave unacceptable fits: the absorption lines they predict are too narrow to reproduce the features visible in the EPIC spectra.

[1]PN version 6.1 epn_sw20_sdY9_medium, epn_sw20_sY9_medium; MOS m1_med_v9q20t5r6_all_15.rsp, m2_med_v9q20t5r6_all_15.rsp

Acceptable fits could only be obtained by adding to the models two absorption lines, which for simplicity we modeled with Gaussian profiles. As shown in Table 1, the line parameters are only slightly dependent on the model adopted for the continuum. The single blackbody yields a lower interstellar absorption, while the other models give higher values, closer to the estimates obtained from radio observations (Giacani et al. 2000). Although the blackbody plus power-law gives formally the best fit (see Fig. 2), we believe that this simply reflects the shortcomings of other models alone to reproduce the low energy part of this complex atmospheric spectrum, rather than being evidence for a distinct non-thermal component.

The fit residuals (lowest panel of Fig. 2) show that the broad lines have a profile characterized by the presence of significant sub-structure. Deviations from a smooth gaussian profile are seen at ∼0.6 keV, ∼0.75 keV and ∼0.85 keV. Although the exact significance of such features is difficult to quantify, this may imply that the broad absorption below 1 keV is produced by blending of several narrower lines.

Another interesting feature is shown by the residuals near 2 keV. This was also noticed in the *Chandra* spectrum by Sanwal et al. (2002), who could not exclude an instrumental effect. The fact that the same line is possibly present in the *XMM-Newton* data, even if at low significance, indicates that it might be really present in the source.

We performed a similar spectral analysis based on the data from the two MOS cameras. This led to results entirely consistent with the ones discussed above, but with larger uncertainties caused by the lower counting rate. All the strongest spectral features were clearly visible in both CCDs.

2.3. Phase-resolved spectroscopy

To search for possible phase-dependent spectral variations, we divided the PN data in four sets corresponding to the phase intervals indicated by the vertical lines in Fig. 1. The resulting spectra were fitted with blackbody models, keeping the absorption fixed at the best fit value of the average spectrum (N_H=3×10^{20} cm^{-2}). While similar temperatures were obtained in the four phase intervals, the fit residuals (Fig. 3) clearly indicate that the absorption features are phase-dependent. In particular the line at ∼1.4 keV is virtually absent at the pulse peak and is more pronounced during the minimum and the rising parts of the pulse profile (see Table 2). Shape variations are also visible for the lower energy feature, which shows a variable sub-structure, suggesting that several narrow lines contribute differently at the various phases.

3. Discussion

The *XMM-Newton* observation confirms the presence of spectral features in the spectrum of 1E 1207–5209 , as recently reported by Sanwal et al. (2002), and allows us to study them in more detail. In particular, both the PN and the two MOS spectra indicate that the feature at ∼0.7 keV cannot be well described by a single gaussian line due to the presence of significant substructure. The PN spectra show phase-dependent variations, particularly pronounced for what concerns the intensity and width of the line at ∼1.4 keV. The presence of phase-dependent variations, leads to the obvious, but important conclusion that the lines are linked to the rotating neutron star and not due to absorption in the line of sight.

According to Sanwal et al., an interpretation of these spectral features in terms of cyclotron resonance lines is difficult, considering the magnetic field inferred from the $\dot{P}$ measurement, B∼3×10^{12} G, and the relative intensity of the two lines. This view has been criticized by Xu et al. (2002), who considered the possibility that 1E 1207–5209 be a bare strange star, spinning down in the propeller regime due to the presence of a fossil disk.

Considering the conventional scenario of an isolated neutron star, a more likely possibility, also suggested by the structured and phase-dependent profiles seen with EPIC, is that these features result from atomic transitions. Pavlov et al. (2002b) interpret them as HeII lines in a strong magnetic field (B∼$(1.4–1.7)\times10^{14}$ G), and derive for the neutron star a radius to mass ratio of (8.8–14.2) km $M_{\odot}^{-1}$. However, such a magnetic field is much higher than the value $(3\pm0.6)\times10^{12}$ G estimated, assuming magnetic dipole braking, from the spin-down value (now confirmed by the *XMM-Newton* data). This implies either that the observed $\dot{P}$ is affected by glitches and/or significant timing noise (and the true spin-down is of the order of $\dot{P}\sim 6\times10^{-11}$ s s^{-1}) or that field components stronger than the dipole are present on (some region of) the neutron star surface (e.g. due to an off-centered dipole).

Alternatively, the lines can be due to heavier elements in a more conventional magnetic field. For example, models of magnetized (B $\gtrsim 10^{12}$ G) iron atmospheres (Rajagopal, Romani & Miller 1997) predict, for temperatures $\sim 10^6$ K, many absorption lines due to atomic transitions in the range above 0.3 keV. Owing to the magnetic field and temperature variation across the neutron star surface, these lines will probably be blurred. Indeed, the results of our phase-resolved spectroscopy show that different physical conditions, most likely due to changing magnetic field configurations, are present on the neutron star regions responsible for the emission visible at different phases. As a consequence, the physical parameters inferred from the fit to phase-averaged spectra should be taken with some caution. It is also likely that the presence of several atomic absorption lines and edges affect the the parameters of the continuum as derived from medium resolution spectra.

1E 1207–5209 is the only neutron star in which significant X–ray absorption features have been detected so far (excluding of course the bright neutron stars accreting in binary systems). Observations with high statistics and good spectral resolution have been recently carried out for several thermally emitting neutron stars of various classes: the middle aged radio pulsar PSR B0656+14 has a spectrum well described by two blackbody components, without spectral lines in the 0.15–0.8 keV range (Marshall & Schultz 2002). No lines were found in the 8.4 s radio-quiet pulsar RX J0720.4–3125 (Paerels et al. 2001) and in the nearby isolated neutron star RX J1856.5–3754. The latter was observed for more than 500 ks with *Chandra* and its spectrum was found to be well described by a blackbody function with temperature kT_{BB}=61 eV without evidence for any of the spectral lines or edges predicted by the models (Drake et al. 2002). No lines have been detected in the spectra of the Vela pulsar (Pavlov et al. 2001) and of the millisecond pulsar PSR J0437–4715 (Zavlin et al. 2002), which are comparable in quality and statistics to the data presented here. Why is 1E 1207–5209 different from the other cooling neutron stars which have been deeply scrutinized for the presence of lines with negative results?

Before trying to answer this question, we must address the problem of the age of 1E 1207–5209 . In this respect, its association with G 296.5+10.0 is crucial. This SNR has a remarkable bilateral symmetry. The two radio arcs that compose the shell have different curvatures, indicating a larger expansion velocity for the ejecta on the western side. The likely site of the supernova explosion is thus relatively well determined to lie to the east of the geometric center, within $8'$ from the position of the pulsar. The spatial coincidence between the pulsar and the SNR is remarkable, also in view of the relatively small number of such objects at this galactic latitude (b=10°). Furthermore, HI observations of this region (Giacani et al. 2000) indicate a spatial correlation between the two objects also for what concerns their distance. Thus we can consider this as one of the strongest neutron star/SNR association. An age of 7 kyrs has been derived for G 296.5+10.0 (Roger et al. 1988), very different from the pulsar characteristic age $\tau_c = (340 \pm 140)$ kyrs. Although the SNR age estimate depends on several uncertain parameters, like its linear size, initial kinetic energy ($E_{51} \times 10^{51}$ ergs) and the density of the interstellar medium (n cm^{-3}), it is very unlikely that G 296.5+10.0 is older than a few $\times 10^4$ years. For example, even taking the maximum distance of 4 kpc compatible with the HI observations (Giacani et al. 2000) an age of $\gtrsim 100$ kyrs can be obtained only for $(n/E_{51}) \gtrsim 1$. This would require a very small initial kinetic energy, since at this distance the SNR would be ∼700 pc above the galactic plane, where the interstellar density is expected to be very small. In conclusion, we believe that a distance of ~ 2 kpc and an age of the order of $\sim 10^4$ years are more likely values.

Although we cannot rule out other possibilities (e.g. one or more glitches in the last two years, significant timing noise, or a faint binary companion), the simplest explanation

to reconcile τ_c with a young age is that 1E 1207–5209 was born spinning at a period close to its current value.

Thus 1E 1207–5209 appears as a unique example of a young pulsar with a small rotational energy loss. Its rotational energy loss $\dot{E}_{rot} \sim 10^{34}$ erg s^{-1}, is the smallest one of all the radio/X–ray pulsars with reliable SNR's associations (Kaspi & Helfand 2002). Such "Crab-like" or "Vela-like" pulsars have typically $\dot{E}_{rot} > 10^{36}$ erg s^{-1} and X–ray luminosity in the range 10^{32}-10^{37} erg s^{-1} (see, e.g., Possenti et al. 2002). Indeed, no plerion has been detected either in radio or X–rays, nor any hint has been found of high-energy γ-ray emission from our object. On this ground, the comparison with the similar age Vela pulsar is striking: beside being active as a radio pulsar, Vela is also the brightest source in the sky at E>100 MeV, and is powering a bright radio/X–ray synchrotron nebula. If the lines are the signature of the presence of metals in the atmosphere, their absence in the older objects mentioned above can be explained by a small layer of hydrogen accreted, even at a modest rate from the interstellar medium over a time span of a few hundred kyrs. The absence of lines (or the difficulty to detect them) in young but energetic pulsars like Vela could be due to the perturbing effects of the non-thermal particles accelerated in the magnetosphere.

4. Conclusions

The *XMM-Newton* observations reported here show unambiguously that the absorption features also seen with *Chandra* (Sanwal et al. 2002) in the X–ray spectrum of 1E 1207–5209 are phase-dependent. Moreover, the lines have significant structures, supporting an interpretation in terms of atomic transitions in regions with different temperature and magnetic field on the neutron star surface. A detailed analysis of phase-resolved spectra with higher statistical quality will undoubtedly provide important information on the surface composition and other important neutron star parameters.

The period value reported here is identical, within the uncertainties, to that obtained two weeks later (Pavlov et al. 2002a), but our smaller error reduces the uncertainty on the pulsar spin-down rate $\dot{P}=(1.98\pm0.83)\times10^{-14}$ s s^{-1}. Since the association with the relatively young SNR remnant is reasonably certain, we consider the high characteristic age of 1E 1207–5209 as evidence that this pulsar was born with a long period.

We suggest that the combination of a young age and a low level of magnetospheric activity are favorable conditions for the detection of atomic spectral features from metals in neutron star atmospheres, which would be either blanketed by a thin layer of accreted hydrogen in older objects or masked by non-thermal processes in young energetic pulsars.

If this scenario is correct, the most promising candidates for line detection are the central X–ray sources in young supernova remnants which do not show synchrotron nebulae, like Cas A, Puppis A, and G 266.1–1.2.

REFERENCES

Becker W. & Trümper J. 1997, A&A 326, 682.

Bignami G.F., Caraveo P.A. & Mereghetti S. 1992, ApJ 389, L67.

Caraveo P.A., Bignami G.F. & Trümper J. 1996, A&AR 7, 209.

Drake J.J. et al. 2002, ApJ 572, 996.

Gänsicke B.T., Braje T.M. & Romani R.W. 2002, A&A, 386, 1001.

Giacani E.B. et al. 2000, AJ 119, 281.

Kaspi V.M. & Helfand D.J. 2002, in *Neutron Stars in Supernova Remnants*, ASP Conference Series, P.O. Slane & B.M. Gaensler, eds., in press

Leahy D.A. 1987, A&A, 180, 275.

Marshall H.L. & Schulz N.S. 2002, submitted to ApJ Letters,

Mereghetti S., Bignami G.F. & Caraveo P.A. 1996, ApJ 464, 842.

Paerels F. et al. 2001, A&A 365, L298.

Pavlov G.G. et al. 2001, ApJ 552, L129.

Pavlov G.G. et al. 2002a, ApJ 569, L95.

Pavlov G.G. et al. 2002b, BAAS 200, 80.01.

Possenti A., Cerutti R., Colpi M. & Mereghetti S. 2002, A&A 387, 993.

Rajagopal R., Romani R.W. & Miller M.C. 1997, ApJ 479, 347.

Roger R.S. et al. 1988, ApJ 322, 940.

Sanwal D., Pavlov G.G., Zavlin V.E & Teter M.A. 2002, ApJ in press.

Strüder L. et al. 2001, A&A 365, L18

Treves A., Turolla R., Zane S. & Colpi M. 2000, PASP 112, 297.

Turner M.J.L. et al. 2001, A&A 365, L27.

Vasisht G. et al. 1997, ApJ 476, L43.

Xu R.X., Wang H.G. & Qiao G.J. 2002, astro-ph/0207079

Zavlin V.E., Pavlov G.G. & Shibanov Yu.A. 1996, A&A 315, 141.

Zavlin V.E. & Pavlov G.G. 2002, in *Proc. 270 Heraeus Seminar on Neutron Stars, Pulsars and Supernova Remnants*, eds. W. Becker, H. Lesch & J. Trümper, astro-ph/0206025

Zavlin V.E., Pavlov G.G., Sanwal D. & Trümper J. 2000, ApJ 540, L25.

Zavlin V.E., et al. 2002, ApJ 569, 894.

Table 1: *Results of PN fits including absorption lines*

	Blackbody + 2 Gaussians	Blackbody + Power law + 2 Gaussians	H atmosphere + 2 Gaussians
N_H (10^{20} cm^{-2})	$3.0^{+1.5}_{-1.2}$	10^{+4}_{-3}	9^{+2}_{-1}
kT (keV)	0.244±0.005	0.219±0.008	0.096±0.005
$R^{(a)}_{BB}$ (km)	1.7±0.2	2.1±0.3	13±1
α_{ph}	–	$2.9^{+0.4}_{-1.2}$	–
E_1 (keV)	0.74±0.02	$0.73^{+0.2}_{-0.6}$	$0.71^{+0.02}_{-0.04}$
σ_1 (keV)	0.13±0.03	0.12±0.04	0.12±0.04
EW_1 (eV)	-90^{+30}_{-60}	-92^{+30}_{-120}	-91^{+15}_{-60}
E_2 (keV)	1.36±0.03	1.36±0.02	1.37±0.02
σ_2 (keV)	0.10±0.05	0.08±0.04	0.07±0.03
EW_2 (eV)	-107^{+36}_{-90}	-67^{+29}_{-54}	-63^{+20}_{-30}
$F^{(b)}_{0.3-3keV}$ (erg cm^{-2} s^{-1})	1.96×10^{-12}	1.96×10^{-12}	1.95×10^{-12}
$F^{(c)}_{PL}$ (erg cm^{-2} s^{-1})	–	5.5×10^{-13}	–
$L^{(d)}_X$ (erg s^{-1})	1.15×10^{33}	1.17×10^{33}	1.8×10^{33}
χ^2/dof	1.54	1.10	1.16
dof	75	73	75

[a] Radius at infinity for an assumed distance of 2 kpc.

[b] Observed flux.

[c] Observed flux of the power law component only, 0.3-3 keV.

[d] Bolometric luminosity (excluding the power law component) for d=2 kpc.

All the errors are at the 90% c.l. for a single interesting parameter

Table 2: *Results phase resolved spectroscopy*

	A	B	C	D
	0.8–1.	0–0.25	0.25–0.55	0.55-0.8
N_H (10^{20} cm^{-2}) fixed	3.0	3.0	3.0	3.0
kT (keV)	0.241±0.004	0.250±0.004	0.245±0.004	0.242±0.004
$R_{BB}^{(a)}$ (km)	1.8	1.7	1.6	1.7
E_1 (keV)	0.78±0.04	0.76±0.04	0.74±0.02	0.71±0.02
σ_1 (keV)	0.12±0.02	0.16±0.04	0.13±0.02	0.08±0.02
$r_1^{(b)}$	0.29±0.08	0.28±0.08	0.35±0.07	0.37±0.11
E_2 (keV)	1.36±0.04	1.37±0.03	1.37±0.02	1.35±0.02
σ_2 (keV)	$0.16^{+0.09}_{-0.04}$	0.18±0.04	0.09±0.02	0.06±0.02
r_2	0.19±0.09	0.30±0.08	0.52±0.13	0.56±0.16
χ^2/dof	1.39	1.00	1.48	1.31
dof	63	68	69	67

[a] Radius at infinity for an assumed distance of 2 kpc.

[b] Relative line depth = 1. – F (E_{line}) / F_C (E_{line}), where F is the total flux and F_C is the flux of the continuum only

All the errors are at the 90% confidence level for a single interesting parameter

Fig. 1.— EPIC PN light curve of 1E 1207–5209 for three different energy ranges. The vertical lines in the top panel indicate the intervals used for the phase-resolved spectroscopy.

Fig. 2.— Fit of the PN data with a blackbody plus power law and two gaussian lines. In the upper panel the data are compared to the model folded through the instrumental response. The middle panel shows the residuals in units of sigma. The lower panels shows the residuals obtained by removing the lines from the model.

Fig. 3.— Phase resolved spectroscopy. The four panels show the residuals of blackbody fits with N_H fixed at 3×10^{20} cm^{-2} for the phase intervals labeled on Fig. 1.

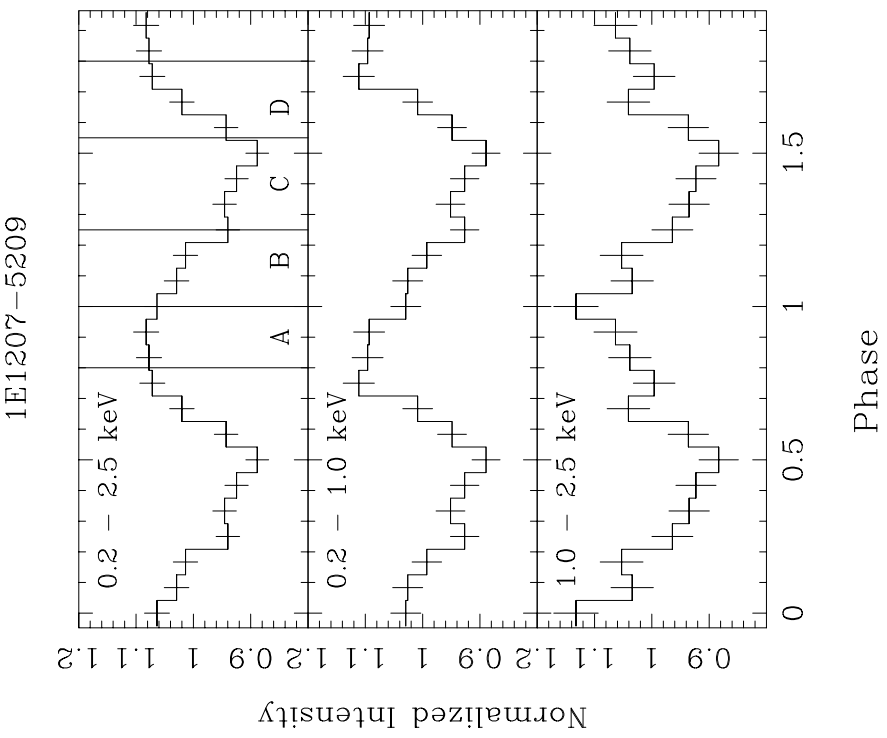
1E1207−5209
0.2 − 2.5 keV
0.2 − 1.0 keV
1.0 − 2.5 keV
A
B
C
D
Normalized Intensity
Phase
0.9
1
1.1
1.2
0
0.5
1
1.5

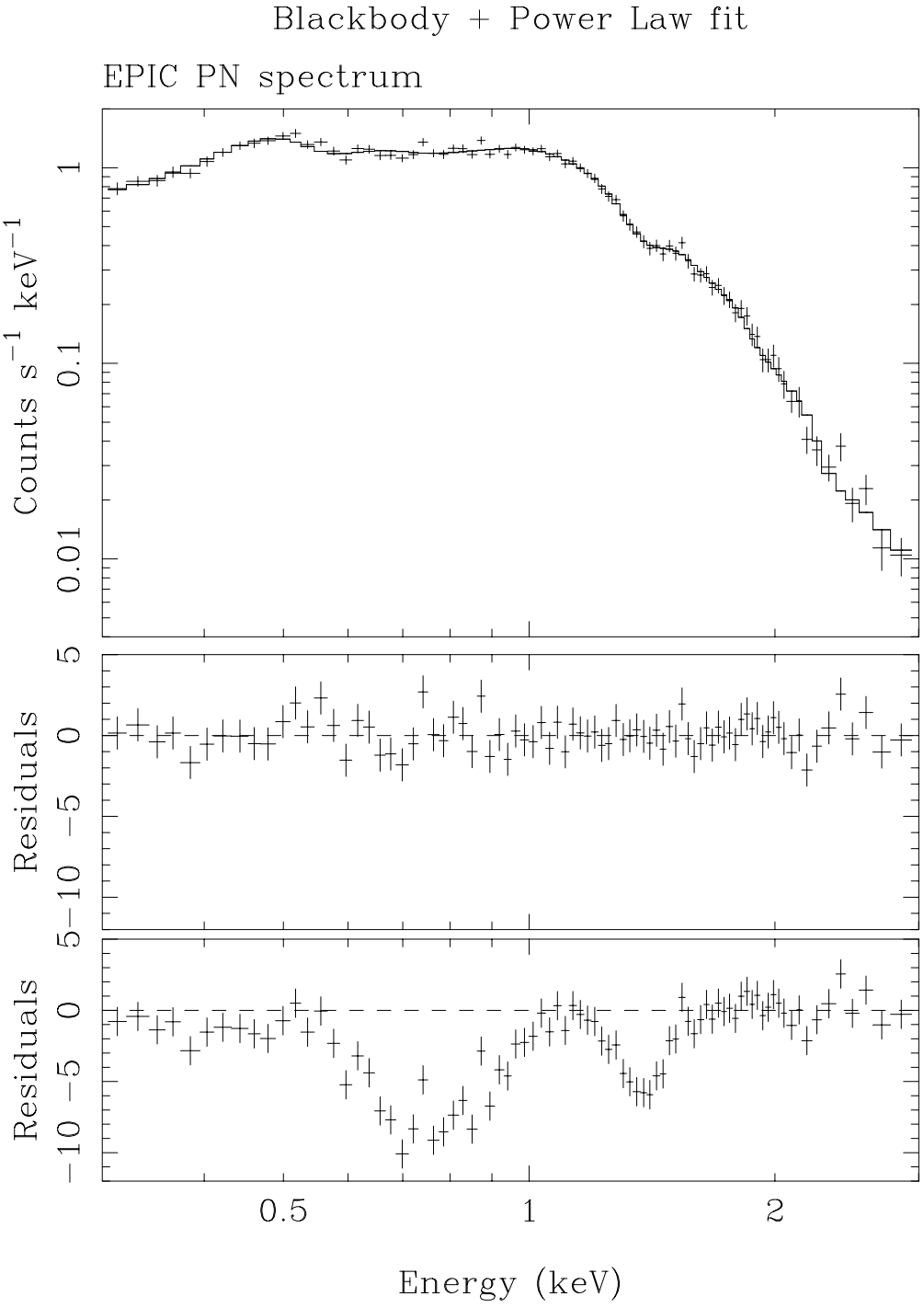
Blackbody + Power Law fit
EPIC PN spectrum
Counts s^{-1} keV^{-1}
1
0.1
0.01
Residuals
5
0
−5
−10
Residuals
5
0
−5
−10
0.5
1
2
Energy (keV)

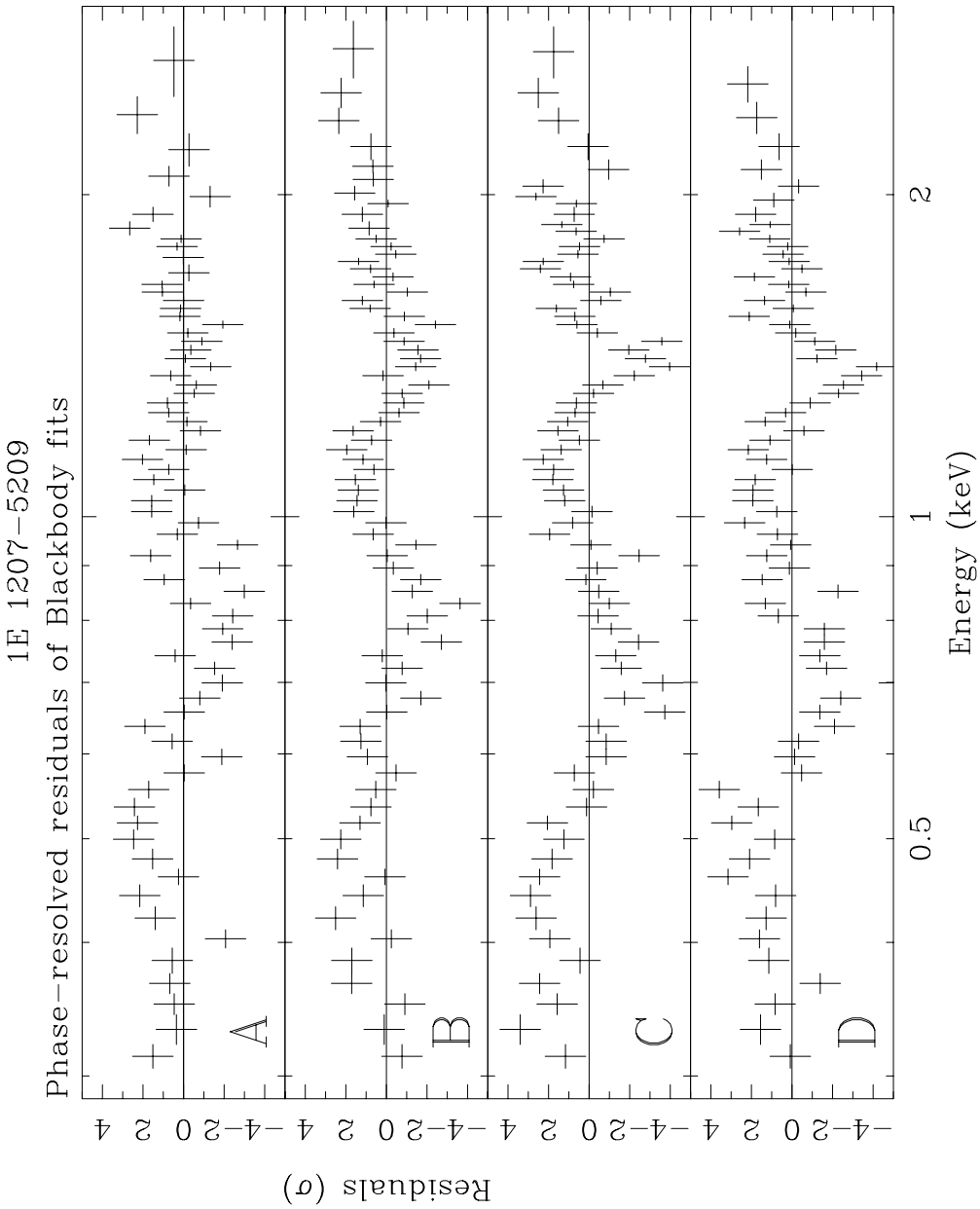
1E 1207−5209
Phase−resolved residuals of Blackbody fits
Residuals (σ)
Energy (keV)
A
B
C
D
0.5
1
2
−4
−2
0
2
4